molecular pharmaceutics

articles

Diacyllipid Micelle-Based Nanocarrier for Magnetically Guided Delivery of Drugs in Photodynamic Therapy

Ludmila O. Cinteza,[†] Tymish Y. Ohulchanskyy,[†] Yudhisthira Sahoo,[†] Earl J. Bergey,[†] Ravindra K. Pandey,[†,‡] and Paras N. Prasad*[,†]

Institute for Lasers, Photonics and Biophotonics, SUNY at Buffalo, Buffalo, New York 14260, and Photodynamic Therapy Center, Roswell Park Cancer Institute, Buffalo, New York 14263

Received February 14, 2006

Abstract: We report the design, synthesis using nanochemistry, and characterization of a novel multifunctional polymeric micelle-based nanocarrier system, which demonstrates combined function of magnetophoretically guided drug delivery together with light-activated photodynamic therapy. Specifically, the nanocarrier consists of polymeric micelles of diacylphospholipid-poly-(ethylene glycol) (PE-PEG) coloaded with the photosensitizer drug 2-[1-hexyloxyethyl]-2-devinyl pyropheophorbide-a (HPPH), and magnetic Fe_3O_4 nanoparticles. The nanocarrier shows excellent stability and activity over several weeks. The physicochemical characterizations have been carried out by transmission electron micrography and optical spectroscopy. An efficient cellular uptake has been confirmed with confocal laser scanning microscopy. The loading efficiency of HPPH is practically unaffected upon coloading with the magnetic nanoparticles, and its phototoxicity is retained. The magnetic response of the nanocarriers was demonstrated by their magnetically directed delivery to tumor cells in vitro. The magnetophoretic control on the cellular uptake provides enhanced imaging and phototoxicity. These multifunctional nanocarriers demonstrate the exciting prospect offered by nanochemistry for targeting photodynamic therapy.

Keywords: Photodynamic therapy; magnetic nanoparticles; polymeric micelles; magnetophoretic control of cellular uptake

Introduction

Nanochemistry offers exciting opportunities for design and fabrication of a wide variety of nanocarriers with multiple applications for nanomedicine, an emerging interdisciplinary field that utilizes nanostructures for diagnostics, targeted drug delivery, and real-time monitoring of therapeutic functions. To achieve these goals of nanomedicine, there is need for development of multifunctional nanocarriers. This paper reports design, synthesis, characterization, and demonstration of multifunctionality of novel polymeric micellar nanocarriers. These carriers provide magnetophoretic control for targeted drug delivery and are designed to produce photodynamic therapeutic action at the targeted site.

Photodynamic therapy (PDT) is considered an innovative and attractive modality to treat localized and superficial tumors, as an alternative to classical therapies such as surgery, radiotherapy, and chemotherapy. Though originally developed for cancer therapy, its potential for application has substantially extended to many noncancer related clinical applications.[1−7] The general procedure for PDT involves the administration of a photosensitizer (PS) followed by its

* Corresponding author. Mailing address: 428 Natural Science Complex, State University of New York at Buffalo, Buffalo, NY 14260-3000. E-mail: pnprasad@buffalo.edu. Tel: 716 645 6800 ext 2098. Fax: 716 645 6945.

† SUNY at Buffalo.

‡ Roswell Park Cancer Institute.

(1) Levy, J. G.; Obochi M. *J. Photochem. Photobiol.* **1996**, *64*, 737−739.

(2) Bonnett, R. *Chemical Aspects of Photodynamic Therapy*; Gordon & Breach: Amsterdam, 2000.

10.1021/mp060015p CCC: $33.50
Published on Web 04/19/2006

irradiation with light of appropriate wavelength and power. The activated PS transfers its excited-state energy to nearby oxygen molecules, leading to the production of reactive oxygen species (ROS) such as molecular oxygen in the excited singlet state ($^1O_2$, singlet oxygen) or free radicals. The ROS molecules are responsible for the cytotoxic action of PDT, where singlet oxygen is the most effective.[8]

However, like many chemotherapeutic drugs, the photosensitizers have limited solubility in water, thus requiring a suitable pharmaceutical formulation for any parenteral administration (e.g., micelles, liposomes, polymeric and ceramic-based nanoparticles, prodrugs, etc.).[9−11] In addition, although some of the photosensitizers show certain intrinsic tumor specificities,[8] their accumulations in skin and other non-neoplastic tissues can still occur. The result is unwanted photodamage of adjacent normal tissues during the treatment. On the basis of these shortcomings, development of novel approaches is still desired for enhancing drug delivery in PDT.

Micelles are nanosized, aqueous self-aggregates of amphiphilic molecules with a hydrophobic core which is capable of solubilizing nonpolar molecules. Therefore, they are attractive carriers of poorly water soluble therapeutic drugs. In PDT, recent preclinical and clinical formulations have used micelles composed of Cremophor-EL, Tween-80, etc.[12−17] However, such micelles disassemble easily upon dilution and are also known to be associated with allergic reactions. As an improvement over surfactant-based micelles, in terms of safety and efficiency, polymeric micelles (PMs) made up of biocompatible, hydrophobic−hydrophilic copolymers (e.g., poloxamers, ploxamines, pluronics, etc.) are being increasingly investigated in the preclinical stage of PDT drug delivery.[18−20] The size of PMs (less than ∼100 nm in diameter), as well as their biocompatible composition, provides them with a prolonged systemic circulation time, due to the capacity to avoid renal exclusion and their reduced uptake/degradation by the reticuloendothelial system. Drugs encapsulated within PMs usually exhibit higher passive accumulation in tumors compared to free drugs with reduced distribution in nontargeted areas.[18−20] This passive accumulation is due to the enhanced permeability and retention effect (EPR) associated with tumor tissues.

Recently, PMs based upon diacyllipid-poly(ethylene glycol) composite molecules have attracted significant attention in drug delivery due to their many unique characteristics. These micelles not only are much smaller (diameter ∼ 20 nm) than other PMs but also are stable at extremely low concentrations.[31] Also, in addition to their increased advantage of EPR-mediated passive tumor accumulation, these micelles can be actively targeted to tumor and other desired sites via conjugation with targeting ligands, including tumor-specific monoclonal antibodies, resulting in increased therapeutic efficacy.[21] However, active targeting using antibody-conjugated carriers still has many disadvantages, such as the lack of deep penetration in the tumor mass, restricted activity against only those tumor cells that express the corresponding antigen, and, most importantly, induced immunogenicity.[22,23] These limitations of antibody−drug conjugates sometimes

(3) Dougherty, T. J.; Gomer, C. J.; Henderson, B. W.; Jori, G.; Kessel, D.; Korbelik, M.; Moan, J.; Peng, Q. *J. Natl. Cancer Inst*. **1998**, *12*, 889−905.

(4) Prasad, P. N. *Introduction to Biophotonics*; Wiley: New York, 2003.

(5) Meisel P.; Kocher T. *J. Photochem. Photobiol. B* **2005**, *79*, 83−170.

(6) Demidova, T. N.; Hamblin, M., R. *Int. J. Immunopathol. Pharmacol.* **2004**, 17, 245−254.

(7) Wilson B. C. *J. Craniofacial Surg.* **2003**, *14*, 278−283.

(8) Allison, R. R.; Downie, G. H.; Cuenca, R.; Hu, X.-H.; Childs, C. J.; Sibata, C. H. *Photodiagn. Photodyn. Ther.* **2004**, *1* (1), 27−42.

(9) Konan, Y. N.; Gurny, R.; Allemann, E. *J. Photochem. Photobiol. B* **2002**, *66*, 89−106.

(10) Roy, I.; Ohulchanskyy, T. Y.; Pudavar, H. E.; Bergey, E. J.; Oseroff, A. R.; Morgan, J.; Dougherty, T. J.; Prasad, P. N. *J. Am. Chem. Soc.* **2003**, *125*, 7860−7865.

(11) Yan, F.; Kopelman, R. *Photochem. Photobiol.* **2003**, *78* (6), 587−591.

(12) Patel, S.; Datta, A. *Chem. Phys. Lett.* **2005**, *413*, 31−35.

(13) Rancan, F.; Helmreich, M.; Molich, A.; Jux, N.; Hirsch, A.; Roder, B.; Witt, C.; Bohm, F. *J. Photochem. Photobiol. B* **2005**, *80*, 1−7.

(14) Gomes, A. J.; Lunardi, L. O.; Marchetti, J. M.; Lunardi, C. N.; Tedesco, A. C. *Drug Delivery* **2005**, *12*, 159−64.

(15) de Oliveira, C. A.; Machado, A. E. H.; Pessine, F. B. T. *Chem. Phys. Lipids* **2005**, *133*, 69−78.

(16) Zhang, G.-D.; Harada, A.; Nishiyama, N.; Jiang, D.-L.; Koyama, H.; Aida, T.; Kataoka, K. *J. Controlled Release* **2003**, *9*, 141−150.

(17) Tijerina, M.; Kopeckova, P.; Kopecek, J. *Pharm. Res*. **2003**, *20*, 728−737.

(18) Torchilin, V. P. *J. Controlled Release* **2001**, *73*, 137−172.

(19) Kataoka, K.; Harada, A.; Nagasaki, Y. *Adv. Drug Delivery Rev.* **2001**, *47*, 113−131.

(20) Neradovic, D.; van Nostrum, C. F.; Hennink, W. E. *Macromolecules* **2001**, *34*, 7589−7591.

(21) Lukyanov, A. N.; Gao, Z.; Torchilin V. P. *J. Controlled Release* **2003**, *91*, 97−102.

(22) van Dongen, G. A. M. S.; Visser, G. W. M.; Vrouenraets, M. B. *Adv. Drug Delivery Rev.* **2004**, *56*, 31−52.

(23) Sharman, W. M.; van Lier, J. E.; Allen, C. M. *Adv. Drug Delivery Rev.* **2004**, *56*, 53−76.

(24) Lubbe, A. S.; Bergemann, C.; Brook, J.; McClure, D. G. *J. Magn. Magn. Mater.* **1999**, *194*, 149−155.

(25) Lubbe, A. S.; Alexiou, C.; Bergemann, C. *J. Surg. Res.* **2001**, *95*, 200−206.

(26) Sahoo, Y.; Goodarzi, A.; Swihart, M. T.; Ohulchanskyy, T. Y.; Kaur, K.; Furlani, E. P.; Prasad P. N. *J. Phys. Chem. B* **2005**, *109*, 3879−3885.

(27) Levy, L.; Sahoo, Y.; Kim, K. S.; Bergey, E. J.; Prasad, P. N. *Chem. Mater.* **2002**, *14*, 3715−3721.

(28) Henderson, B. W.; Bellnier, D. A.; Graco, W. R.; Sharma, A.; Pandey, R. K.; Vaughan, L.; Weishaupt, K.; Dougherty, T. J. *Cancer Res*. **1997**, *57*, 4000−4007.

(29) Bellnier, D. A.; Greco, W. R.; Loewen, G. M.; Nava, H.; Oseroff, A. R.; Pandey, R. K.; Tsuchida, T.; Dougherty, T. J. *Cancer Res.* **2003**, *63*, 1806−1813.

(30) Sun, S.; Zeng, H. *J. Am. Chem. Soc.* **2002**, *124*, 8204−8205.

(31) Wang, J.; Mongayt, D.; Torchilin, V. P. *J. Drug Targeting* **2005**, *13*, 73−80.

make the simple passive targeting a safer and better approach in drug delivery.

An ambitious goal of drug delivery is to externally "remotely control" the drug carriers in order to achieve the goal of maximum target specificity. One way to achieve this is by the introduction of magnetic properties in the drug carriers, followed by manipulating the pharmacodynamics of the carrier with an external magnetic field. This approach seems highly feasible for magnetically accessible tumors, which, coincidently, are targets for PDT. Magnetic materials like iron oxide nanoparticles have long been successfully used in a number of biomedical applications[24−27] and are not likely to evoke any additional biosafety issues for the composite nanocarriers. Therefore, developing a nanocarrier codoped with photosensitizers and magnetic nanoparticles and externally controlling their accumulation at target sites, followed by light irradiation, is expected to significantly enhance the therapeutic efficacy. Recently, Kopelman et al. have combined the commercially available PDT drug PHOTOFRIN and an MRI agent in a polymeric nanoparticle system that enabled the dual purpose of MRI and therapy. They successfully demonstrated both MRI and PDT treatment with iron oxide and PDT drug containing polymeric nanoparticles in vivo.[34] However, no magnetophoretic control study was reported. Jain et al. have shown entrapment of the hydrophobic drug doxorubicin within the ligand layer on the surface of iron oxide nanoparticles where the formulation was stabilized in water by oleic acid and pluoronic F-127 surfactant.[35] In another related work, Kim et al. have demonstrated the formation of stable aqueous dispersion of organically prepared iron oxide particles by using block copolymer micelles.[36] In this work, we report the development of a novel diacyllipid-poly(ethylene glycol) PM based nanocarrier system, coencapsulating the PS 2-[1-hexyloxyethyl]-2-devinyl pyropheophorbide-a (HPPH)[28,29] and magnetite nanoparticles. The merits of our approach include (i) ability to incorporate the presynthesized, monodispersed magnetic particles organosol, which can be extended to many other magnetic particles besides Fe_3O_4; (ii) enhanced load density of the magnetic and drug fractions; and (iii) long shelf life because of the good thermodynamic stability of polymeric micelles. The loading of the magnetite nanoparticles had little effect on the loading efficiency of HPPH, and light irradiation of the composite nanocarriers resulted in a robust PDT-mediated cytotoxic effect on tumor cells in vitro. We also demonstrate the controllability of this nanocarrier with the external magnetic field and the feasibility of the magnetic guidance for the enhanced cellular uptake of the nanocarrier in vitro.

Experimental Section

Materials. 1,2-Distearoyl-*sn*-glycero-3-phosphoethanolamine-*N*-[methoxy(poly(ethylene glycol))-2000] (ammonium salt) (PEG-2000-DSPE) and 1,2-dioleoyl-*sn*-glycero-3-phosphoethanolamine-*N*-carboxyfluorescein) (fluorescein-PE) were purchased from Avanti Polar Lipids. Iron acetyl acetonate, oleic acid, hexadecanediol, and phenyl ether were purchased from Sigma-Aldrich. Dimethyl sulfoxide (DMSO) is a product of Fisher Chemicals. Deuterium oxide (D_2O) was purchased from Cambridge Isotope Laboratories.

The photosensitizer, 2-[1-hexyloxyethyl]-2-devinyl pyropheophorbide-a (HPPH), was kindly provided by the Roswell Park Cancer Institute. Cell culture products, unless mentioned otherwise, were purchased from GIBCO. The HeLa cell line was obtained from American Type Culture Collection. Cells were cultured according to instructions supplied by the vendor.

Magnetic Nanoparticle Synthesis and Characterization. The magnetic nanoparticles used in this study were Fe_3O_4 nanoparticles that were prepared by adaptation of the reported procedure by Sun et al.[30] In a typical reaction, 1 mmol of iron acetylacetonate, 3 mmol of oleic acid, 5 mmol of 1,2-hexadecanediol, and 20 mL of phenyl ether were taken together in a three-necked flask, and the mixture was heated at 265 °C for 90 min. The particles were first isolated from the crude product by precipitation through addition of acetone/ethanol and centrifugation. The precipitate could be readily redispersed by adding any of the solvents such as chloroform, toluene, or hexane.

Nanocarrier Preparation and Characterization. Polymeric diacyllipid micelles were prepared from PEG-2000-DSPE according to the methodology previously described by Torchilin.[18] A modified procedure was used to prepare complex micelle-based nanocarriers, coencapsulating magnetic particles and PS. Briefly, 20 mg of polymeric lipid derivative was dissolved in chloroform, and various volumes of a stock solution of magnetic nanoparticle dispersions in chloroform (concentration $\sim$ 1.8 g/mL) and/or HPPH solution (15 μM in DMSO) were added. Each resulting dispersion was sonicated for 5 min with a Cole Parmer 700 W ultrasonicator in pulse mode (0.2 s) in an ice bath. After the removal of the organic solvent under reduced pressure, the lipidic film, deposited on the vial walls, was rehydrated in water and subjected to a further ultrasonication for 10 min using a bath sonicator. The resulting micellar solution was filtered through a 0.2 μm cutoff SFCA membrane filter (Corning Co., NY) before any use. For in vitro interactions with cells and stability studies, the micelles were resuspended in phosphate buffer saline PBS at pH 7.4. For the imaging studies, fluorescent-labeled-micellar nanocarriers were prepared by adding 1% (w/w) fluorescein-PE (λ_{abs} = 497 nm; λ_{em} = 521 nm) to the micelle-forming mixture in chloroform.

(32) Anderson, T. M.; Dougherty, T. J.; Tan, D.; Sumlin, A.; Schlossin, J. M.; Kanter, P. M. *Anticancer Res.* **2003**, *23*, 3713−3718.
(33) Balasubramaniam E., Natarajan P. *J. Photochem. Photobiol. A: Chem.* **1997**, *103*, 201−211.
(34) Kopelman, R.; Koo, Y.-E. L.; Philbert, M.; Moffat, B. A.; Reddy, G. R.; McConville, P.; Hall, D. E.; Chenevert, T. L.; Bhojani, M. S.; Buck, S. M.; Rehemtulla, A.; Ross, B. D. *J. Magn. Magn. Mater.* **2005**, *293*, 404−410.
(35) Jain, T. K.; Morales, M. A.; Sahoo, S. K.; Leslie-Pelecky, D. L.; Labhasetwar, V. *Mol. Pharm.* **2005**, *2*, 194−205.
(36) Kim, B. S.; Qiu J. M.; Wang J. P.; Taton, T. A. *Nano Lett.* **2005**, *5*, 1987−1991.

The size distribution and surface potential of pure micelles and the micelle-based nanocarriers were determined by dynamic light scattering (DLS) measurement with a Brookhaven Instruments 90Plus particle size analyzer, with a scattering angle of 90° and particle size range measurements of 2 nm to 3 μm. The measurements were repeated five times, and each size data represents an average of five sequences of 5 runs. For the ζ potential measurement, a phase analysis light scattering (PALS) module was used, with the software based on the Smoluchowski theory. For each sample 5 runs with 10−15 cycles each were performed. An average value was finally obtained from the five measurements. In all DLS experiments, diluted samples, both in water and in 0.1 M NaCl solution, were used.

The morphology of the particles was determined using images obtained by TEM for diluted samples spread on holey carbon and Formvar film coated copper grids. A transmission electron microscope (JEOL TEM 2020) operating at an accelerating voltage of 200 kV was employed for the measurement of the sizes and shapes of the pristine magnetic nanoparticles and those coencapsulated with the PS. The micelle solutions were stained with phosphotungstic acid at a final concentration ~0.01 wt %. A drop of the stained micelle solutions was then placed on a copper grid and was self-dried in a drybox at 20 °C.

The concentration of the drug in the freshly prepared nanocarriers and in stability study samples was determined by absorption spectroscopy, using the molar extinction coefficient of HPPH (ϵ = 47 500 M^{-1} cm^{-1} at 665 nm).

Efficiency of the Magnetic Material and Photosensitizer Encapsulation. To quantitatively analyze the amount of drug and magnetic nanoparticles entrapped in the micellar nanocarriers, 1 mL of dispersion, freshly prepared and filtered through a 0.2 μm SFCA membrane filter (Corning Co, NY), was taken. Nonincorporated HPPH, similar to other water-insoluble crystalline drugs under normal circumstances, cannot pass through the filter, unless the drug is solubilized in a suitable nanoscale formulation. To remove any trace of organic solvent and free drug, the polymeric micelles were cleaned by dialysis against distilled water (1 L) for 48 h, the water phase being replaced every 2 h during the first 24 h, and then every 6 h. The concentration of HPPH in various formulations was determined by spectroscopic measurement of a diluted sample in DMSO. The concentration of magnetic material was determined by thermogravimetric analysis.

Storage Stability. In order to study the influence of each component on the stability of the formulation, the nanocarrier samples were loaded in three distinct fashions: (i) with HPPH alone, (ii) with magnetic nanoparticles alone, and (iii) with both HPPH and magnetic nanoparticles. All three samples were stored under standard conditions, in the dark, at 4 °C for 4 weeks. The stability of the formulation was appreciable as there were no changes in the size and the size distribution of the polymeric micelles. Also, no loss of encapsulated magnetic particles and HPPH was observed during the storage.

Release of the Photosensitizer. The release kinetic profile of HPPH was investigated at 37 °C using the dialysis method. Briefly, 1 mL of each micelle-based nanocarrier, loaded as previously described, was placed in a molecular porous dialysis membrane (SpectraPor, regenerate cellulose), molecular weight cutoff size 3500 Da. Dialysis was performed against 1 L of distilled water that was replaced every 12 h, after a withdrawal of 50 μL of the sample from the nanocarrier dispersion. The sample was further diluted with DMSO and used for determination of HPPH using the spectrophotometric method described above.

Optical Spectroscopy. The UV−vis absorption spectra were recorded in a quartz cuvette with a 1 cm path length, using either a Shimadzu UV-3101PC spectrophotometer or a Hewlett-Packard 8452A spectrophotometer. The fluorescence spectra were taken on a Fluorolog-3 spectrofluorometer (Jobin Yvon, Longjumeau, France). A SPEX 270M spectrometer (Jobin Yvon) equipped with an InGaAs photodetector (Electro-Optical Systems Inc.) was used for the acquisition of singlet oxygen emission spectra. Spectra were acquired for samples in D_2O because of extended singlet oxygen lifetime in D_2O in comparison with water. A diode-pumped solid-state laser (Verdi, Coherent) at 532 nm was the excitation source. Long-pass filters, 538AELP and 950 LP (Omega Optical), were used to attenuate the excitation laser light and fluorescence from the samples.

In Vitro Studies with Tumor Cells: Nanoparticle Uptake, Imaging, and Viability Assay. For studying micelle uptake and imaging, the cells were trypsinized and resuspended in a MEM alpha medium with 10% fetal bovine serum (FBS) at a concentration of 7.5 × 10^5 cells/mL and plated in 60 mm culture plates, using 5 mL of the medium containing 0.10 mL of the cell suspension. The plates were incubated overnight at 37 °C with 5% CO_2. On the next day, the cells (50% confluency) were carefully rinsed with phosphate-buffered saline (PBS), and 5 mL of the medium containing 50 μL of the aqueous dispersion of polymeric micelles was added to each plate and mixed gently. The treated cells were returned to the incubator for 90 min. For magnetophoretic control on uptake, the treated culture dish was placed on the top of a 0.5 T magnet (20 mm diameter) and incubated overnight as above. The plates were rinsed with sterile PBS, and fresh medium was added. The cells were then directly imaged using a confocal laser scanning microscope (MRC-1024, Bio-Rad, Richmond, CA). A water immersion objective lens (Nikon, Fluor-60X, NA = 1.0) was used for cell imaging. A Ti:sapphire laser (Tsunami from Spectra-Physics) pumped by a diode-pumped solid-state laser (Millenia, Spectra Physics) was used as a source of excitation of HPPH emission. The Ti:sapphire output, tuned to 840 nm, was frequency doubled by second harmonic generation (SHG) in a β-barium borate (β-BBO) crystal to obtain the 420 nm light, and was coupled into a single mode fiber for delivery into the confocal scan head. A long-pass filter, 585 LP (585 nm), and an additional band-pass filter with transmission at 680 ± 15 nm (Chroma 680/30) were used as emission filters for imaging HPPH fluorescence. To image polymeric micelles labeled with fluorescein, the 488 nm line of an argon ion laser (Spectra-Physics) was used. A band-

pass filter, 522/30, was used to image fluorescence from the fluorescein-labeled micelles.

The phototoxic effect of the polymeric micelle-based HPPH-containing formulation on cell viability was estimated by means of the colorimetric MTT assay[10] (see Supporting Information).

Results and Discussion

Magnetic Targeting Micelle-Based Nanocarriers. Fe_3O_4 nanoparticles produced by the hot organic colloidal route are monodiperse, with an average diameter of 8 nm and with ~10% size distribution. The particles are magnetic and evidently show attraction to the magnetic field when they are in the form of a slurry, a powder, or an unstable dispersion. In a very concentrated or a destabilized dispersion, the dipolar forces among the particles dominate and the response to magnetic field can be observed. It should be noted that, in a stabilized dispersion, the magnetic attraction of the particles does not seem apparent, because the Brownian motion afforded by the stable dispersion overcomes any magnetic attraction.

Poly(ethylene glycol) modified by attaching diacyllipid residues (phosphatidylethanolamine, PE) was used to prepare the nanocarrier by loading it with magnetic nanoparticles and PS. The polymeric PEG corona of the formed micelles should ensure the long-term circulating properties of the nanocarrier, acting as a protection against the fast removal from the blood stream by the reticuloendothelial system (RES).

This PEG−lipid conjugate, containing PEG, with molecular weight 2000 Da and stearoyl phospatidyl ethanolamine, was chosen to ensure an optimum balance between the hydrophobic drug encapsulation capacity and prevention of uptake by phagocytic cells. Polymeric micelles prepared from the derivative with PEG 2000 chains possess suitable long-time circulating properties;[18,21] stearoyl lipid was found to be most suitable for the delivery of PS, among the derivatives based on PEG 2000 with different alkyl chains, because it renders the highest size of the hydrophobic core.

To find an optimum condition for coencapsulation of the magnetic nanoparticles and HPPH in the desired therapeutic amounts, a series of nanocarriers was prepared by entrapping various load ratios of magnetic nanoparticles and HPPH.

The size and ζ potential of plain polymeric micelles were found to be 13.2 nm and −30.2 mV, respectively, similar to those reported by other authors.[20,31] The encapsulation of HPPH does not significantly change the size and size distribution of the PEG-2000-PE micelles, as shown in Table 1. Incorporation of the magnetic nanoparticles in high concentration (above 30% w/w in total solid content) affects the size of the polymeric micelles more significantly, but still the final size of the nanocarrier remains under 50 nm, favorable for the EPR effect discussed above.

The size distribution for highest content of magnetic nanoparticles was shown to be broader than that of the original sample of void micelles. High concentration of encapsulated magnetic nanoparticles (over 35% w/w in solid content) results in a larger size of nanocarrier and higher polydispersity, due to aggregation of the magnetic nanoparticles inside the core of the micelle (Figure 1).

Table 1. Average Size and Surface Potential of PEG-2000-PE Nanocarriers[a]

nanocarrier composition	size (nm)	polydispersity index	surface potential (mV)
PEG-2000-PE	13.2 ± 2.5	0.005	−30.2 ± 2.8
PEG-2000-PE loaded with HPPH	18.7 ± 5.8	0.006	−26.8 ± 2.1
PEG-2000-PE loaded with magnetic nanoparticles	24.5 ± 7.8	0.246	−25.2 ± 4.5
PEG-2000-PE loaded with HPPH and magnetic nanoparticles	34.8 ± 7.2	0.310	−23.5 ± 3.9

[a] Concentration of HPPH in nanocarrier dispersion 12 mM. Concentration of magnetic nanoparticles 30% w/w in total solid content of nanocarrier dispersion.

Whereas the size of the void micelles has a median diameter of ~18 nm as seen in Figure 1A, the micelles loaded with magnetic particles show a distinct population of swollen sizes. The second peak at ~150 nm in Figure 1B corresponds to structures formed by micelle aggregation at higher concentration. These aggregates are not stable and could be easily redispersed by simply shaking or sonicating the sample.

The surface potential of the micellar carrier increases with an increase in the content of both the PS and the magnetic material entrapped (Table 1), which can be attributed to a change in the surface/volume ratio of the micelle at the same composition. The critical micellar concentration (CMC) of the PEG-2000-DSPE is approximately 50 mg/L at room temperature in phosphate buffer, which allows formulations that remain stable by surviving dilutions during the administration.[18] Studies of the dilution effect on the stability of the PS entrapped in polymeric micelles were performed in PBS, by checking the drug retention in stock micellar dispersions (diluted 500- and 700-fold). No significant change in the relative amount of drug encapsulated in the micellar core was observed in both the dilution experiments, affirming a high degree of stability of the PEG-PE polymeric micelles (data not shown).

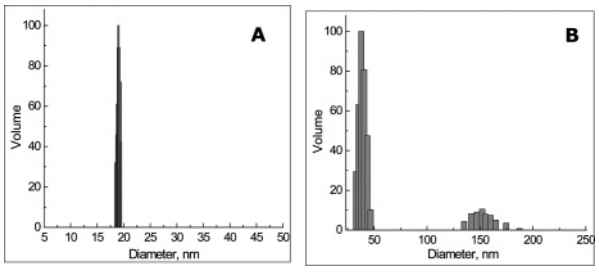

Figure 1. (A) Size distribution of micellar based nanocarriers loaded with PS HPPH alone. (B) The same with coencapsulated magnetic nanoparticles, 30% w/w.

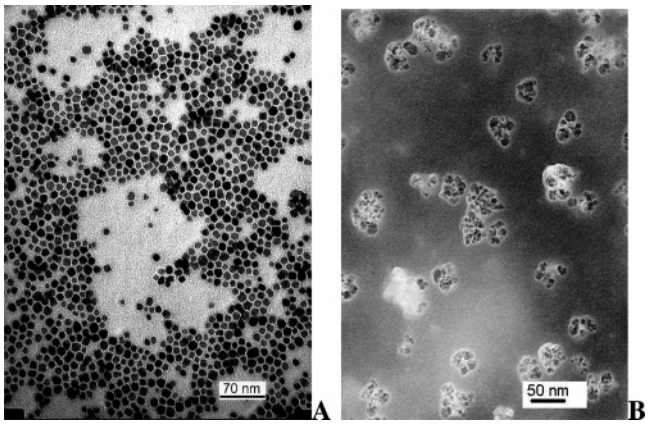

Figure 2. TEM image of the (A) magnetic nanoparticles from toluene dispersion and (B) magnetic nanoparticles within the polymeric micelles.

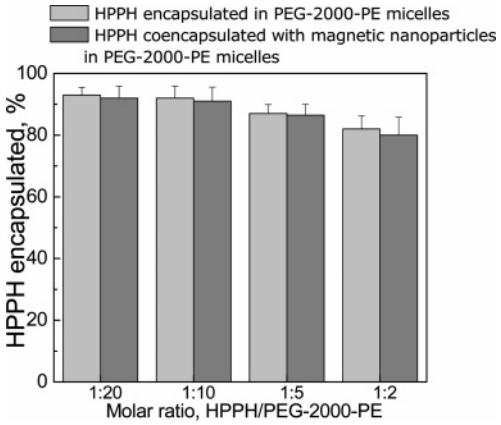

Figure 3. Encapsulation of the photosensitizer HPPH in polymeric diacyllipid-based nanocarrier with and without magnetic material added.

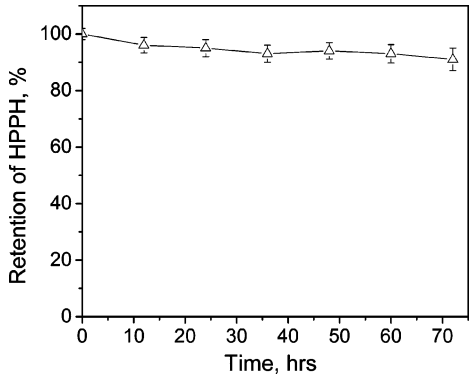

Figure 4. The retention of HPPH in PEG-2000-PE magnetic polymeric micelles (10% magnetic material w/w) in PBS, pH = 7.4 at 37 °C.

The morphology of the nanocarriers was determined by TEM (Figure 2). Figure 2A depicts the image of the pristine magnetic nanoparticles from toluene dispersion. As can be seen, these particles are reasonably monodispersed, with ~10% size distribution, and remain discrete.

In Figure 2B is imaged the polymeric micelle with a 30% load of magnetic particles that was diluted and negatively stained with phosphotungstic acid solution to enhance contrast, which allows visualization of magnetic nanoparticles as dark spots and polymeric micelles as a light surrounding circular area. However, it was noted that, up to 10% (w/w) load fraction, the magnetic particles show discrete morphology in the TEM (not shown here), as in the case of pristine particles. Between 10% and 30% w/w load fractions, the clustering of magnetic nanoparticles inside the micellar core systematically increases and leads to a broader size distribution of the nanocarriers (Table 1, Figure 2B). This suggests that 10% load fraction is a critical limit up to which the particles can singly occupy a micellar cavity.

The encapsulation of the magnetic nanoparticles was examined in samples prepared by variation in relative (w/w) concentration of the magnetic material in the solid content of the dispersion (drug + diacyllipid polymer + magnetic nanoparticles). It was found that, for the range of 10−30% (w/w) of magnetic nanoparticles, up to 90% of the initial magnetic material was successfully incorporated in the polymeric micelles, while maintaining nanocarrier stability. The HPPH encapsulation efficiency was evaluated for different w/w ratios of the drug to polymeric diacyllipid (Figure 3).

Up to a 1:10 molar ratio of drug to polymer compound, the efficiency of drug encapsulation was over 90%. The efficiency of HPPH entrapment decreases with a decrease in the HPPH to polymeric diacyllipid ratio (from above 90% at 1:20 to ~80% at 1:2). Even at this lower encapsulation efficiency, it is possible to prepare the drug delivery system with a concentration of about 12 mM, significantly higher than those of a typical formulation used in preclinical studies (2 mM in Tween-80 aqueous solution−ethanol mixture).[32] At a content of up to 30% magnetic nanoparticles (w/w in micelle-forming solid material), the entrapment of HPPH is not significantly affected by the presence of magnetic material (Figure 3).

The release kinetics of the encapsulated drug from the PEG-2000-PE polymeric micelles in PBS, at 37 °C, is presented in Figure 4. In 72 h, the polymeric micellar formulation, loaded with HPPH at a 1:2 w/w drug:polymer ratio, loses less than 10% from the initial drug content, most of it being in the first 12 h. The high retention of HPPH in polymeric micelle-based nanocarrier clearly demonstrates that the incorporated PS is strongly associated with the encapsulating material, reducing the risk of drug loss during transport to the tumor.

The retention of HPPH is not affected by the presence of magnetic nanoparticles in the micelle for up to 30% content in magnetic nanoparticles. The carrier, coencapsulating PS and magnetic nanoparticles, demonstrates good retention of both entrapped materials; thus it is possible to use it for delivery and magnetically guide the PS to the tumor tissue, without a significant loss of both active components.

The formulations based on HPPH-loaded PEG-2000-PE micelles with and without magnetic nanoparticles were investigated for stability under short-term conditions (samples were stored in the dark for 4 weeks, at 4 °C). There were no noticeable changes in the sizes of the micelles for the stored

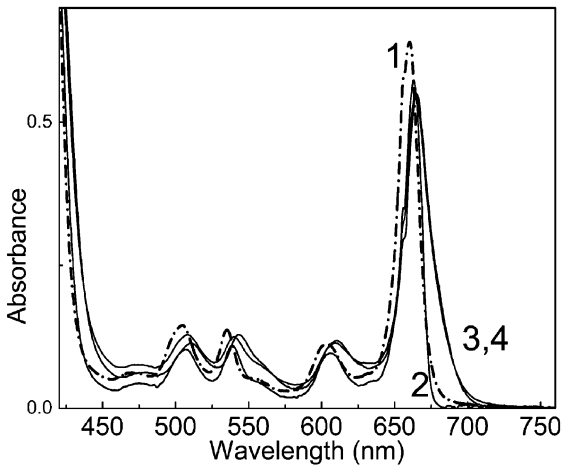

Figure 5. UV−vis spectra of HPPH in various media: (1) DMSO; (2) Tween-80; (3) PEG-PE; (4) PEG-PE loaded with magnetic nanoparticles.

suspension, in comparison with that for the freshly prepared samples. Aggregates of micelles were found present for both cases, which could be redispersed by sonication.

The relative decrease of content of the HPPH encapsulated in the stored samples is ∼2.8% and ∼2.5% for the formulations with and without magnetic nanoparticles, respectively. Both polymeric micelle-based formulations, with and without magnetic content, exhibit good stability of the nanocarrier under storage conditions used for the pharmaceutical products.

Photophysical Properties of HPPH-Loaded Magnetic Nanocarriers. The absorption spectra of HPPH in the DMSO solution and the micellar dispersion in Tween-80 and the PEG-2000-PE nanocarrier are presented in Figure 5. The spectra of HPPH in Tween-80 and in polymeric diacyllipid are red shifted in comparison with the DMSO solution, due to the entrapment of the PS inside the micelle core. This bathochromic shift is known for different chromophores embedded in microheterogeneous media.[33]

It is worth noting that there is a similar difference between the absorption of HPPH encapsulated in Tween-80 micelles and that in PEG-2000-PE micelles. Notably, the presence of the magnetic nanoparticles does not significantly affect the optical absorption properties of HPPH (Figure 5).

The fluorescence emission spectra of HPPH in Tween-80 and in polymeric diacyllipid micelles are shown in Figure 6. In contrast to free HPPH, which loses fluorescence in water, HPPH in PEG-2000-PE maintains its fluorescent properties, similar to HPPH in Tween-80. Some decrease in the intensity of HPPH fluorescence in PEG-PE micelles, in comparison with HPPH in Tween-80, was observed. HPPH, being a nonpolar molecule, aggregates in polar solvents; consequently its fluorescence is self-quenched. As long as the HPPH molecules are dispersed within the nonpolar cores of the micelles, they remain isolated and exhibit a high fluorescent signal. However, in contact with more polar surrounding media (PEG corona is a region of hydrated polymer), aggregation occurs, resulting in a decrease of fluorescence.

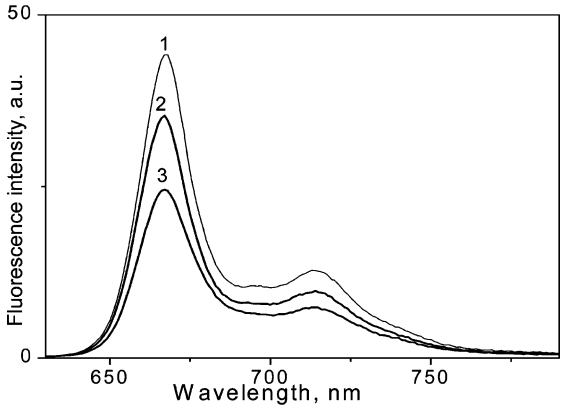

Figure 6. Fluorescence emission spectra of HPPH in Tween-80 micelles (1) and in PEG-PE-based nanocarriers with (2) and without magnetic nanoparticles (3). Absorbance was matched at the wavelength of excitation (532 nm).

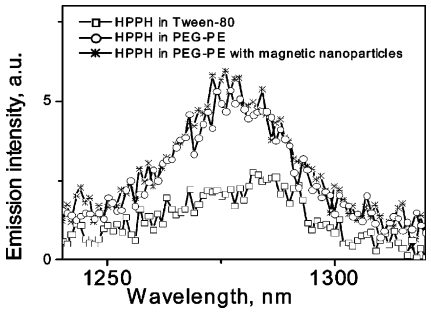

Figure 7. Emission spectra of singlet oxygen generated by HPPH in Tween-80 micelles (squares) and in PEG-PE-based nanocarriers with (stars) and without magnetic nanoparticles (circles). Absorbance of HPPH was matched at the wavelength of excitation (532 nm). D_2O suspensions.

If the decrease in the HPPH fluorescence intensity in PEG-PE micelles in comparison with HPPH in Tween-80 is due to higher aggregation, one can expect also a decrease in singlet oxygen generation in micelles. The singlet oxygen generation efficiency for HPPH in different micellar systems was compared. As one can see in Figure 7, HPPH in PEG-PE micelles shows a higher singlet oxygen generation efficiency compared to HPPH in Tween-80. It could be because of an enhanced stability of polymeric micelles under excitation of HPPH or a higher rate of molecular oxygen diffusion through the PEG-PE micelle shell. Notwithstanding the actual reason, it is important to note that HPPH entrapped in the PEG-PE micelles exhibits significant value for singlet oxygen generation efficiency, similar to or even higher than HPPH in Tween-80 used currently as a pharmaceutically accepted formulation. Additionally, these results show that the optical properties of PS in PEG-PE micelles are not compromised to any significant extent by the presence of magnetic material coencapsulated with the PS.

Cellular Uptake in Vitro. The cellular uptake of the diacyllipid-based nanocarrier by the cells incubated with fluorescent-modified micelles was determined using confocal microscopy. The dye-lipid conjugate 1,2-dioleoyl-*sn*-glycero-3-phosphoethanolamine-*N*-(carboxyfluorescein) was used to

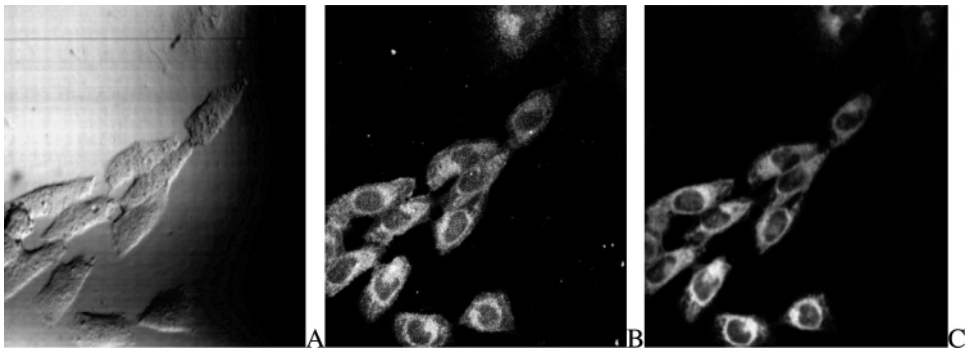

Figure 8. Confocal microscopy images of Hela cells after 90 min of incubation with fluorescent PEG-2000-PE micelles loaded with HPPH: (A) transmission; (B) fluorescence from fluorescein-labeled micelles; (C) fluorescence from HPPH.

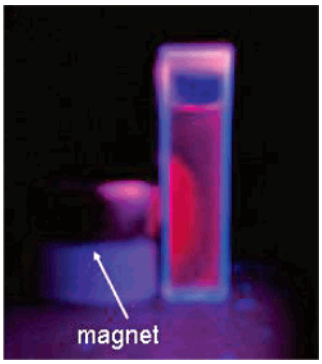

Figure 9. Fluorescent PEG-2000-PE micelles attracted by the magnet. Red fluorescence of HPPH is seen. UV excitation (365 nm) from a UV torch was used.

prepare fluorescent-labeled micelles. This dye was chosen to provide a clear spectral separation of fluorescence from the fluorescent-labeled micelles and fluorescence from entrapped PS (fluorescence maxima at ∼520 nm for the fluorescein derivative and 665 nm for HPPH).

As seen in Figure 8, HPPH entrapped in PEG-PE micelles was successfully taken up by the cells. Localization of HPPH inside the cells is similar to that of fluorescent micelles (Figure 8B,C), showing that PEG-PE micelles retain HPPH in cells, following 90 min of the treatment. Thus, the similarity of the distribution patterns obtained for fluorescence from fluorescein-labeled micelles and those from encapsulated HPPH allows us to conclude that micellar nanocarriers remain stable enough to retain HPPH during incubation with cells in medium and after cellular uptake. It is worth noting that the viability of treated cells was verified by their morphology, and it indicated that the cells were found in good condition even after staining overnight.

The polymeric micelle-based nanocarrier containing HPPH also exhibits phototoxic efficiency similar to that of HPPH-loaded Tween-80 micelles, both in the presence and in the absence of magnetic particles (see Supporting Information). In general, it can be concluded that the loading of HPPH in the polymeric micelles, PEG-PE (with and without magnetic nanoparticles), is at least as effective a drug/carrier system as HPPH solubilized in Tween-80 micelles for killing tumor cells in vitro.

Magnetophoretic Control and Guidance of Cellular Uptake by an External Magnetic Field. The entrapment of magnetic nanoparticles inside polymeric micelles leads to the formation of a nanocarrier with a capability of

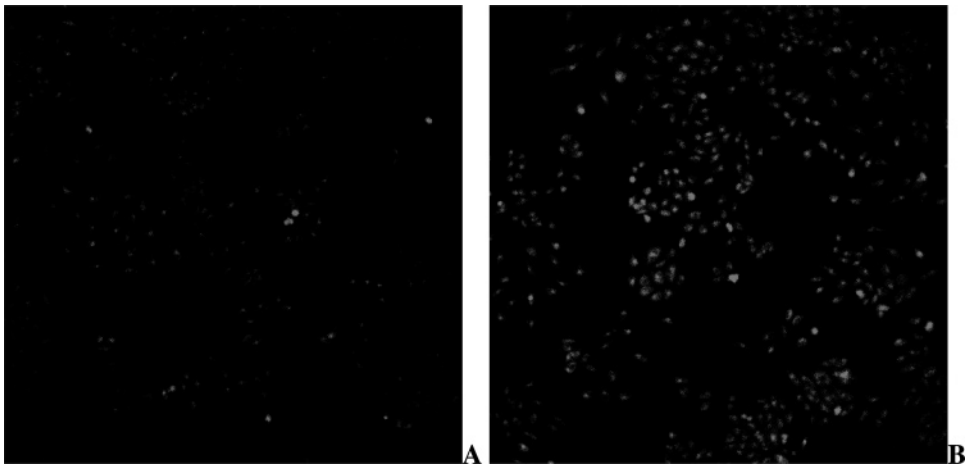

Figure 10. Fluorescence microscopic images of cells stained with PEG-PE micelles coentrapping HPPH and magnetic nanoparticles: (A) cell dish area outside of the area where magnet was applied and (B) inside that area. Detector gain and confocal pinhole were kept the same. Fluorescence intensity was maximized in both cases by selecting focal plane with maximum of fluorescence.

magnetic response to an external magnetic field. We have observed this response by juxtaposing a magnet with a cuvette containing a dispersion of the fluorescent magnetic micelles containing HPPH, as shown in Figure 9, and keeping it overnight. As one can see, magnetic micelles containing fluorescent HPPH were attracted by the magnet and concentrated near the cuvette wall next to the magnet.

This unequivocally illustrates that the PS is intimately coencapsulated with the magnetic particles, for otherwise such a PS luminescence gradient would not be observed. As an extension of this experiment, the possibility of magnetically guiding the polymeric micelles to enhance the uptake in the targeted area was tested using cell cultures selectively exposed to an external magnetic field. HPPH-containing polymeric magnetic micellar dispersion was added to a cell dish and properly mixed. Then the dish was located on the top of a magnet and kept overnight. Then confocal fluorescence images were taken from the locations inside the area where the magnetic field was applied, as well from the area outside it. As it is seen in Figure 10, where two such fluorescence images are presented, there is a clear difference in HPPH uptake between the area where the magnet was applied and the areas outside. It not only unambiguously shows a possibility to magnetophoretically control the cellular uptake, but also provides additional proof of colocalization of HPPH and magnetic nanoparticles in micellar nanocarriers during cellular treatment and uptake. It is worth also noting that used cell medium contains 10% of FBS, to some extent mimicking physiological conditions.

Conclusions

In summary, we have developed a novel nanocarrier system which makes possible magnetically guided delivery of drugs to target cells. The high stability of polymeric micelle-based nanocarriers themselves and high retention of drug allow us to consider that the new nanocarrier can deliver drug without any significant loss in the blood circulation. The photophysical properties and in vitro efficacy of the encapsulated drug remain unaltered upon magnetic nanoparticle coencapsulation. We have shown that the coencapsulation of PDT drug with magnetic nanoparticles provides an ability to magnetically guide PDT drug as well as to enhance drug accumulation in desired area. Thus, incorporating a magnetic moiety in a nanocarrier formulation can unequivocally offer an additional degree of freedom for targeted drug delivery and consequent therapeutic efficacy.

Acknowledgment. This study was supported by NIH Grants CA104492 and CA55791. We also acknowledge support from the John Oishei Foundation, University at Buffalo Interdisciplinary Research and Creative Activities Fund and Center for Bioinformatics and Life Sciences. We also thank Lisa A. Vathy for her technical support.

Supporting Information Available: Experimental details and data on phototoxicity study. This material is available free of charge via the Internet at http://pubs.acs.org.

MP060015P